

Establishment of a New Orthotopic Perirenal-Space-Grafted Mouse Model of Retroperitoneal Sarcoma

Fu'an Xie

Xiamen University

Dongmei Qin

Xiamen University Medical College

Lanlan Lian

Xiamen University

Ming Li

Xiamen University

Xu Kong

Xiamen University

Xiaogang Xia

Xiamen University

Liyong Huang

Fuzhou First Hospital

Jun Chen

Peking university international hospital

Chundong Yu (✉ cdyu@xmu.edu.cn)

Xiamen University <https://orcid.org/0000-0002-4141-8345>

Chenghua Luo

Peking University international hospital

Wengang Li

Xiamen University

Research

Keywords: Retroperitoneal sarcoma, Perirenal space, Orthotopic xenotransplantation model

Posted Date: October 14th, 2020


DOI: <https://doi.org/10.21203/rs.3.rs-89811/v1>

License: © ⓘ This work is licensed under a Creative Commons Attribution 4.0 International License.

[Read Full License](#)

Abstract

Background: Retroperitoneal sarcoma is a group of tumour originating from mesenchymal tissue in the retroperitoneal space. Although its incidence is lower than other tumours, retroperitoneal sarcoma has attracted increasing attention due to their high degree of malignancy, high recurrence rate and younger tendency. At present, the available treatments for retroperitoneal sarcoma are limited due to a lack of basic research and appropriate animal models.

Results: In this study, two human sarcoma cell lines (dedifferentiated liposarcoma cell line SW872 and fibrosarcoma cell line HT1080) were selected to establish an orthotopic xenotransplantation retroperitoneal sarcoma mouse model. To achieve this, sarcoma cells labelled with GFP-Luc-Puro tag were inoculated into the perirenal space of nude mice. We evaluated the model by live imaging, histopathology and transcriptome analysis. Doxorubicin and Cisplatin were used to test the response of this model to chemotherapy drugs. The abdominal bulge of mice was obvious after 15 days for HT1080 and 30 days for SW872. Obvious chemical signals could be detected by an imaging system (IVIS Lumina ) , and a solid tumour was visible in the abdominal cavity of live mice by MRI in vivo. Solid tumours inoculated in the perirenal space were significantly larger than subcutaneous tumours. Moreover, solid tumours treated with doxorubicin and cisplatin were significantly smaller than those treated with PBS. Through transcriptome analysis, we found several signal pathway associated with tumorigenesis including TNF and NF- κ B signaling pathways. Notably, a significant increase in copy number of MDM2 and a significant reduction in TP53, consistent with a shift in the MDM2/TP53 axis, with the most decisive genomic event contributing to liposarcoma development.

Conclusions: In summary, we successfully established an orthotopic xenotransplantation model of retroperitoneal sarcoma, which can be used to study the initiation and development of retroperitoneal sarcoma, drug screening, diagnostic methods and new surgical procedures.

Introduction

Soft tissue sarcomas (STS) are a heterogeneous group of rare malignancies with mesenchymal origin that arise in any anatomic site. They account for almost 1.5% of all human malignant tumours, with an increased incidence in younger adults[1, 2]. The retroperitoneum is the primary site of 15–20% of STS[3, 4]. Moreover, the retroperitoneal location is often associated with a worse prognosis than STS in other locations. Among the retroperitoneal sarcomas (RPS), malignant retroperitoneal sarcoma (MRPS) accounts for about 80% of cases. However, all sarcoma subtypes can arise at this location. The most common histotypes of RPS are well-differentiated/dedifferentiated liposarcoma, solitary fibrous tumours, leiomyosarcoma, undifferentiated pleomorphic sarcoma and malignant peripheral nerve sheath tumours. RPS originating in this anatomic location are usually hidden deep in the retroperitoneum. They tend to reach large sizes and often encase or infiltrate multiple adjacent organs before they become symptomatic[5]. It is difficult to complete radical resection for these tumours, and the recurrence rate is

high[6]. Because MRPS are not sensitive to radiotherapy and chemotherapy[7], the treatment and prognosis of MRPS represents a common global challenge in the field of oncology.

There are limited advancements in diagnosis and treatment options available to RPS patients compared to other cancers due to a lack of basic and clinical research, especially appropriate cell and animal models[8]. Current retroperitoneal sarcoma models include cell-derived xenograft (CDX), patient-derived xenograft (PDX) and transgenic animal models. SICD mice was used for patient-derived subcutaneous xenograft[9–15]. Athymic nude NMRI mice was used for subcutaneous xenograft[16]. Assi et al.[17] employed intramuscular injection of human SW872 cells. Jason M. Warram et al.[18] implanted HT1080 into the posterior of female nude athymic mice. Daniel Johannes Tilkorn et al.[19] placed a tissue engineering chamber around the vessels. In addition to xenograft, some scholars have established a retroperitoneal tumor model at the genetic level. Gutierrez A et al. use active myristoylated Akt2, administered through microinjection with a DNA construct carrying Akt2, which synergizes with p53 loss to drive liposarcoma genesis in zebrafish[20]. Bi P et al. found that activated Notch signalling in mature adipocytes elicited dedifferentiated liposarcoma (DDLPS) formation via the suppression of Ppar- γ function[21]. Wang Z et al. observed well-differentiated liposarcoma (WDLPS) when IL-22 was overexpressed in mouse adipocytes [22]. Wu J W et al. found that mice lacking both Atgl and Hsl showed near-complete deficiency of lipolysis and formed liposarcoma tumours between 11 and 14 months of age.

These previously reported PDX, CDX and transgenic animal models have played an important role in the study of retroperitoneal sarcomas, but they are limited in terms of sample acquisition, animal raising, short-term efficiency and the complexity of genetic mutations. The most common model, subcutaneous xenograft, cannot reflect the occurrence and development of tumours to the same extent as orthotopic xenografts. Orthotopic xenograft models provide a more appropriate microenvironment compared to ectopic xenograft models. A simple animal model that closely mimics the real situation with good short-term efficiency is necessary for molecular biology, imaging, drug screening and testing[19].

Here, we performed orthotopic transplantation of the fibrosarcoma cell line HT1080 and liposarcoma cell line SW872 into the retroperitoneal perirenal space to establish a mouse model of retroperitoneal sarcoma with new in situ growth that is easily accessed and presents faster growth and high verisimilitude. This orthotopic xenograft model will serve as a powerful in vivo tool to further understand sarcomagenesis and improve drug screening, diagnostic procedures and the development of therapeutic modalities.

Results

Inoculation of fibrosarcoma HT1080 and liposarcoma SW872 cells into the perirenal space

The anatomic location of the retroperitoneum is the space between the retroperitoneal peritoneum and the abdominal transverse fascia under the diaphragm but above the pelvic diaphragm. Retroperitoneal tumours usually originate in the latent space of the retroperitoneum, including primary retroperitoneal

tumours and metastatic tumours from fat, loose connective tissue, muscle, fascia, blood vessels, nerves and lymphoid tissue in the retroperitoneal space. As shown in Fig. 1A, the retroperitoneal space is marked by the dotted line. We chose the perirenal space for transplantation of HT1080 and SW872 with GFP-Luc-Puro tagged cells, as shown in the position marked by an asterisk (Fig. 1A, B). We injected trypan blue into the perirenal space to highlight the location and post injection effects (Fig. 1B).

HT1080 and SW872 cells exhibit fast growth and tumorigenesis in the retroperitoneal perirenal space.

The tumorigenesis of HT1080 and SW872 cells could be observed after inoculation of the perirenal space with GFP-Luc-Puro tagged HT1080 and SW872 cells (Fig. 2). The luminescence signal was detected and it gradually enhanced with time (Fig. 2A), suggesting that the tumours are established and grow. We also confirmed the tumorigenesis through MRI: a solid tumour with a clear boundary was formed at the site of the asterisk (Fig. 2B). HT1080 or SW872 cells could form obvious solid tumours in the perirenal space within 15 and 30 days, respectively. These mice were dissected after decapitation, and we observed that both fibrosarcoma HT1080 and liposarcoma SW872 cells could form visible solid tumours with a little adhesion to the surrounding organs (Fig. 2C).

Retroperitoneal sarcoma cells inoculated in the perirenal space have stronger tumorigenic ability than inoculated subcutaneously.

Previous studies have reported that it is difficult for retroperitoneal sarcoma cells to form subcutaneous xenograft tumours in nude mice. To examine the differences in tumorigenicity between perirenal space inoculation and subcutaneous inoculation, we injected same amount of HT1080 or SW872 cells in perirenal space and subcutaneous space of nude mice to establish xenograft tumours, respectively. Both HT1080 and SW872 cells inoculated in the perirenal space had stronger tumorigenic ability compared to cells inoculated subcutaneously ($p < 0.001$) (Fig. 3A, B). MDM2 overexpression and its inhibition of p53 activity in the sarcomatous tumour lead to overexpansion of the cells, which may be one of the pathogenic mechanisms underlying RLPS[12, 24]. As a common tumour marker, Ki67 is commonly used as a marker of malignant proliferation. In the current study, extensive Ki67- and MDM2- positive cells were observed in these tumor tissues, suggest that the tumors in current models had basic characteristics of retroperitoneal tumours (Fig. 3C). Meanwhile, Ki67 staining was performed to examine tumor cell proliferation between perirenal space and subcutaneous grafted tumours. Since subcutaneous grafted HT1080 cells formed hydrous pus like masses and could not be dissected, further IHC staining was conducted only on SW872 tumour masses. The results showed that the positive rate of Ki67 staining had no significant difference between perirenal-space-grafted and subcutaneously-grafted tumours (Fig. 3D); however, the TUNEL-positive cells in perirenal-space-grafted tumours were significantly less than those in subcutaneously- grafted-tumours (Fig. 3E). These results suggest that perirenal space is more suitable for the survival but not proliferation of retroperitoneal sarcomas as compared to subcutaneous space.

Compare gene expression between perirenal-space-grafted and subcutaneously-grafted tumours

To further understand why the tumorigenic ability of cells inoculated in the perirenal space was stronger than that in cells inoculated subcutaneously, three solid SW872 tumours formed in the perirenal space

and three solid SW872 tumours formed in subcutaneous space were selected to construct transcriptome sequencing libraries. Whole transcriptome profiling was performed (Fig. 4). The transcriptome data indicated that a total of 18,983 genes were detected in these tumours (see Supplementary table 1). The volcanic map shows gene distribution and gene expression differences (Fig. 4A). 11,061 genes were found to be differentially expressed, of which 5876 genes were upregulated and 5185 were downregulated. We selected 421 genes related to tumour formation or tumorigenesis. There were a total of 217 genes whose variation range reached 1.3 times (Fig. 4B; Supplementary table 2). KEGG pathway classification and enrichment analysis for DEGs were also carried out. A total of 216 genes were allocated to six main KEGG metabolic pathways (Fig. 4C): 22 genes were classified as cellular processes, 30 genes as environment information, 8 genes as genetic information processing, 83 genes as human disease, 32 genes as metabolism, and 55 genes as organismal system pathways. The main secondary pathways were cell growth and death (9), signal transduction(26), folding, sorting and degradation(4), infection diseases-viral(9), global and overview maps(6), and immune system(20). The main altered pathways are TNF signaling pathway, NF-kappa B signaling pathway, Proteasome, NOD-like receptor signaling pathway, IL-17 signaling pathway (Fig. 4D). These changed molecules are mainly involved in regulating cell growth, death and the immune system. Compared with subcutaneously-grafted tumours, the TNF signaling pathway is inhibited in perirenal-space-grafted tumours, which may result in decreased apoptosis. In the NF-kappa B signaling pathway, uPA and P65 are enhanced in perirenal-space-grafted tumours, which may promote cell survival. Genes that significantly up-regulate more than 4 times include PRF1, LAMC2, MAGEA1, AIM2, EMP2, PTPN22, CHRFAM7A, KLF2, KRT15, KRT8, EDA2R, SPHK1, F2RL1, CLU, PTGER4, PLA2, LAMB3, SMAGP, Genes down-regulated by more than 4 times include CXCL1, MMP1, TNFSF11, G0S2, THY1, HSPB1, MBP, IL6, TNFRSF11B, ICAM1, SELENBP1, PYCARD, CD40, UBD1, IRAK3, CLIP3, ADAMTS12, CYBA, VCAM1, etc., see Supplementary table 2 Notably, when perirenal-space-grafted tumours were compared to subcutaneously-grafted tumours, MDM2 expression was upregulated 3.14 times ($p < 0.001$), while TP53 expression was downregulated 1.5 times ($0.01 < p < 0.05$; see Supplementary table 1). MDM2/TP53 was identified as the most decisive pathway associated with liposarcoma development in clinical samples.

Use perirenal-space-grafted tumorigenesis model to evaluate drug therapies for retroperitoneal sarcoma.

Although surgery represents the mainstay for the treatment of localized RPS, doxorubicin is used as the first-line drug in soft tissue sarcomas (STS). Cisplatin is a commonly used chemotherapy drug. We evaluated the response of ps-CDX models to doxorubicin and cisplatin. The therapeutic effect was assessed by examining changes in bioluminescence imaging signaling intensity, tumour weight, and body weight of tumour-bearing mice. We injected 100- μ l DMEM containing 1×10^7 HT1080 fibrosarcoma cells into the perirenal space of each nude mouse, which were divided into three groups: PBS, cisplatin (5 mg/kg), and doxorubicin (4 mg/kg). Mice received intraperitoneal injection of their respective treatment starting from the third day after the initial cell injection, then received subsequent treatments every 3 days. In addition, on day 3, 6, and 15, luciferin signal acquisition was performed using the IVIS Lumina II system. The fluorescence signal intensity of the PBS group gradually increased with

time, and the weight of solid tumours was significantly higher than those of mice in the cisplatin ($p < 0.01$) and doxorubicin ($p < 0.01$) groups (Fig. 5A, B). It is noted that long-term use of cisplatin and doxorubicin resulted in a significant decrease in body weight. (Fig. 5C).

Discussion

Tumours located in the retroperitoneal region often associate with a worse prognosis compared with the tumors located in trunk and limbs. In fact, in this anatomic location, tumours have a tendency to grow to a larger size, associated with a comparatively lower chance of surgical excision. The purpose of this study was to establish a xenograft tumours at the site of origin of retroperitoneal tumours in nude mice to provide a mouse model to study retroperitoneal sarcoma tumorigenesis.

In this study, we successfully established a retroperitoneal orthotopic xenograft model by inoculating liposarcoma and fibrosarcoma cells into primary origin sites of retroperitoneal sarcoma in nude mice. Furthermore, we found that retroperitoneal sarcoma cells inoculated in the perirenal space have stronger tumorigenic ability than inoculated subcutaneously, which is due to better survival in the perirenal space. Through RNA sequencing, we identified a number of signaling pathways that promote the formation of retroperitoneal sarcoma in perirenal-space-grafted tumours altered compared to those in subcutaneously-grafted tumours. Among them, TNF/NF-kappa B and MDM2/TP53 signaling pathways attracted our attention. TNF, as a critical cytokine, can induce a wide range of intracellular signal pathways including apoptosis and cell survival as well as inflammation and immunity[25]. TNFR1 induce activation of many genes, primarily related to two distinct pathways: survival pathway including NF-kappa B and MAPK cascade, and death pathway including apoptosis and necroptosis. TNFR2 signaling activates NF-kappa B pathway including PI3K-dependent NF-kappa B pathway and JNK pathway leading to survival[26]. NF-kappa B is the generic name of a family of transcription factors that function as dimers and regulate genes involved in immunity, inflammation and cell survival[27]. Notably, the MDM2/TP53 axis, which plays a reference role in the study of the mechanism underlying the formation of human retroperitoneal sarcoma. Moreover, in order to verify the practicability of this model, we tested the effects of doxorubicin and cisplatin treatment on the retroperitoneal orthotopic xenograft, verifying that the animal model can be used for evaluating pharmacological effect.

In clinical practice, retroperitoneal tumours are usually large and can crush or invade adjacent organs and blood vessels, such as the kidneys, adrenal gland, spleen and colon[28, 29]. Complete surgical resection is currently recognised as the most effective treatment, but the complete resection rate of primary tumours is still low and the recurrence rate remains high[6]. The primary site of STS has an important impact on the prognosis of patients, as the prognosis of RPS is much worse than tumours located in the limbs or trunk. At present, the scope of resection of RPS remains uncertain. The current debate is focussed on the need to dissect adjacent tissues that cannot be observed by the naked eyes[30]. Although the recurrence rate can be greatly reduced by large-scale whole or extended resection of uninvolved organs, the removal of adjacent organs is also a challenge, associated with increased

complications after organ resection. The predictive ability of surgical resection margin evaluation on post operative complications still needs to be explored[31].

There is no evidence to show that retroperitoneal tumours are sensitive to radiotherapy, chemotherapy or immunotherapy; therefore, postoperative adjuvant therapy is not commonly used [32]. Due to a lack of effective drugs, systemic therapy has failed to play an important role in the treatment of retroperitoneal liposarcoma. In recent years, due to continuing basic and clinical research, some promising clinical exploration prospects have emerged. Molecular targeting and cell therapy have gained attention and become the focus of investigations[33]. The mechanism of retroperitoneal development, accurate preoperative diagnosis, precise intraoperative surgery and precise non-surgical targeted therapy are also under investigation. All the research requires an animal model that closely resembles the real retroperitoneal tumour for preliminary exploration and advancements in technology.

In this study, we report the establishment of an orthotopic xenotransplantation model of retroperitoneal sarcoma. This model has several characteristics. Firstly, it is inoculated in situ, which mimics the environment of retroperitoneal sarcoma occurrence. The model also allows the visualisation of tumour cells due to GFP-Luc labelling, which can reflect the occurrence and development of the tumour more accurately and comprehensively, and can also more accurately reflect the therapeutic effect of drugs. From the anatomical map, it can be seen that the model is closely related to clinical retroperitoneal tumours. Therefore, it can be used to study new surgical procedures and outcomes. It is worth noting that retroperitoneal sarcoma is not sensitive to any of the current chemotherapeutic drugs. This model can be used to verify the effects of newer treatments including cell therapy and immunotherapy, which have emerged in recent years. Secondly, the observed enhancement of the MDM2/TP53 signalling pathway is similar to that observed in the clinic, so this model can be used for the development and exploration of new diagnostic markers and methods. Finally, the mice used in this model are ordinary nude mice, and the cells are commercial cell lines, which provides great advantages in terms of operation, feeding conditions and price compared to severely defective nude mice like SCID mice. Unlike the previous PDX model, tissues do not need to be obtained from patients, which requires extended waiting time for appropriate surgery and strict ethical review. The commercial cell lines used in the current model are easier to obtain.

Conclusion

The present study has demonstrated that sarcoma cells, including fibrosarcoma and liposarcoma cells, can be successfully grafted into the retroperitoneal perirenal space of nude mice. The consistently high engraftment rate and major preservation of immunophenotypes observed indicates that such xenografts can be used as tools in studies aimed at improving our understanding of retroperitoneal sarcoma tumorigenesis. Potential applications of the xenografts include preclinical testing of responses to various chemotherapeutic regimens, evaluation of novel therapeutic agents and diagnostic methods, analysis of tumour progression at the cellular and molecular levels, and identification of new therapeutic targets.

Methods

Cell culture and cell lines

All cells grew under standard incubation condition (37°C, humidified atmosphere, 5% CO₂) and maintained in Dulbecco's Modified Eagle medium (SH 30022.01, Hyclone, USA) supplemented with 10% FBS (1530690, Gibco, USA), 100 U/mL penicillin and 100 U/mL streptomycin (B540732, Sangon, China). Human liposarcoma cell line SW872 and human fibrosarcoma cell line HT1080 were purchased from the American Type Culture Collection (ATCC). The stable expression tag GFP-Luc-Puro was constructed in the PLV-basic vector. Virus stocks were prepared by cotransfecting Plv-GFP-Luc-Puro with two packaging plasmids (pHR and pVSVG) into 293T cells. SW872 and HT1080 cells were infected with viruses carrying GFP-Luc-Puro in the presence of polybrene (8 µg/ml, TR-1003, Sigma-Aldrich German) for 1 day. Infected cells were screened by treatment with Puromycin (20 µg/µl, A606719, Sangon, China) for 1 week.

Animals

Four- to six-week-old athymic nude mice were obtained from the Laboratory Animal Center of Xiamen University. Animals were housed in individually ventilated cages with sterilised food and water under specific pathogen-free conditions in the Laboratory Animal Center of Xiamen University in accordance with international standards. Animals were regularly checked by a certified veterinarian who was responsible for health monitoring, animal welfare supervision and experimental protocols. All experimental procedures involving animals were conducted in accordance with animal protocols approved by the Laboratory Animal Center of Xiamen University and Ethics Committee of Xiamen University (XMULAC20190114).

In vivo animal studies

The RPS orthotopic xenograft mouse model was established by injecting 0.1 ml of tumour cell suspension (DMEM) containing 1×10^7 cells for SW872 and 1×10^5 cells for HT1080 into the perirenal space and subcutaneous space. When the tumour volume reached a palpable size, the mouse was used for further studies.

Immunohistochemistry staining

Tumour sections were cut at a thickness of 5 µm using a microtome and mounted on glass microscope slides. For immunohistochemical staining, sections were dewaxed in xylene and hydrated in graded alcohol solutions and distilled water. Routine haematoxylin and eosin (H&E) staining was carried out. Immunohistochemical staining was performed using antibodies against the proto-oncogene MDM2 (bs23748R, Bioss, China) and proliferation marker Ki67 (15580, Abcam) according to the manufacturers' recommendations.

Bioluminescence imaging

Nude mice bearing SW872 and HT1080 with GFP-Luc-Puro tagged cell orthotopic xenografts were injected with 100 µl of luciferin solution intraperitoneally. The mice were left for 10 min and then anesthetised before imaging. Bioluminescence of live mice was monitored using an in vivo imaging system (IVIS Lumina [®]; Caliper life Science, Hopkinton, MA, USA). The luminescence intensity was quantified as photon counts per second using Living Image software.

MRI imaging

Nude mice bearing SW872 and HT1080 with GFP-Luc-Puro tagged cell xenografts were evaluated by in vivo MRI, as described previously[23].

TUNEL Staining

Briefly, slides (4 mm) were stained with TdT-mediated dUTP nick end labeling (TUNEL) probes (Roche, 11684817910, United States) according to the product instructions. DAPI was used to stain the nuclei. Images were captured using a fluorescence microscope.

RNA sequencing

Transcriptome sequencing was conducted by Wuhan BGI Technology Co., Ltd. Briefly, total RNA was extracted from xenografts in the perirenal space and subcutaneous locations, then the Illumina HiSeq4000 platform RSEM was used for RNA quantification. Based on raw count data, differential expression analysis between samples was performed using the PoissonDis algorithm.

Statistical Analysis

All data were collected from more than three independent experiments, expressed as the mean ± standard error of the mean. All statistical significance was determined by unpaired two-sided t-tests using GraphPad Prism 5. For all figures, differences were considered significant at *p < 0.05, **p < 0.01 and ***p < 0.001.

List Of Abbreviations

soft tissue sarcomas (STS); retroperitoneal sarcoma(RPS); malignant retroperitoneal sarcoma (MRPS); cell-derived xenograft (CDX); patient-derived xenograft (PDX); perirenal-space-cell derived xenograft (ps-CDX); well-differentiated liposarcomas (WDLPS); dedifferentiated liposarcomas (DDLPS)

Declarations

Ethics approval and consent to participate

All mice were raised in the Laboratory Animal Center of Xiamen University. This research study was approved by the Ethics Committee of the Xiang'an Hospital of Xiamen University. All animal experiments

were performed in strict accordance with the relevant laws and regulations approved by the Institutional Animal Care and Use Committee of Xiamen University. All efforts are to minimize the number of animals, minimize the manipulation, and minimize the pain of the animals.

Consent for publication

Not applicable.

Availability of data and materials

All data generated or analyzed during this study are included in this article.

Competing interests

The author declare that he have no competing interests.

Funding

This work was supported by grants from the National Natural Science Foundation of China (No. 81972223 to Wengang Li, No. 81970485 and No. 81772942 to Chundong Yu), the Scientific Research Foundation for Advanced Talents, Xiang'an Hosptial of Xiamen University (NO. PM20180917008 to WL), and the Natural Science Foundation of FuJian province (No. 2018J01366 to Liyong Huang).

Authors' contributions

WL, CL, CY and FX conceived the idea; FX designed the project, conducted experiments, analyzed the data, performed statistical analyses, and wrote the manuscript; QD and LL performed plasmid construction, virus packaging cell culture and bred the mice. XX performed IHC; ML and XK revised the manuscript; JC and LH provided scientific support and professional guidance.

Acknowledgements

The authors would like to thank Haiping Zheng, the experimentalists at Central Laboratory, School of Medicine, Xiamen University for their technical assistance with flow cytometry.

References

1. Gatta, G., van der Zwan, J.M., Casali, P.G., Siesling, S., Dei Tos, A.P., Kunkler, I., Otter, R., Licitra, L., Mallone, S., Tavilla, A., et al. (2011). Rare cancers are not so rare: the rare cancer burden in Europe. *Eur J Cancer* *47*, 2493-2511.
2. Fletcher, C.D. (2014). The evolving classification of soft tissue tumours - an update based on the new 2013 WHO classification. *Histopathology* *64*, 2-11.
3. Bonvalot, S., Rivoire, M., Castaing, M., Stoeckle, E., Le Cesne, A., Blay, J.Y., and Laplanche, A. (2009). Primary retroperitoneal sarcomas: a multivariate analysis of surgical factors associated with local

- control. *Journal of clinical oncology : official journal of the American Society of Clinical Oncology* 27, 31-37.
4. Messiou, C., Moskovic, E., Vanel, D., Morosi, C., Benchimol, R., Strauss, D., Miah, A., Douis, H., van Houdt, W., and Bonvalot, S. (2017). Primary retroperitoneal soft tissue sarcoma: Imaging appearances, pitfalls and diagnostic algorithm. *European journal of surgical oncology : the journal of the European Society of Surgical Oncology and the British Association of Surgical Oncology* 43, 1191-1198.
 5. Chouairry, C.J., Abdul-Karim, F.W., and MacLennan, G.T. (2007). Retroperitoneal liposarcoma. *The Journal of urology* 177, 1145.
 6. Jaques, D.P., Coit, D.G., Hajdu, S.I., and Brennan, M.F. (1990). Management of primary and recurrent soft-tissue sarcoma of the retroperitoneum. *Annals of surgery* 212, 51-59.
 7. Bonvalot, S., Raut, C.P., Pollock, R.E., Rutkowski, P., Strauss, D.C., Hayes, A.J., Van Coevorden, F., Fiore, M., Stoeckle, E., Hohenberger, P., et al. (2012). Technical considerations in surgery for retroperitoneal sarcomas: position paper from E-Surge, a master class in sarcoma surgery, and EORTC-STBSG. *Annals of surgical oncology* 19, 2981-2991.
 8. Dei Tos, A.P. (2014). Liposarcomas: diagnostic pitfalls and new insights. *Histopathology* 64, 38-52.
 9. Stebbing, J., Paz, K., Schwartz, G.K., Wexler, L.H., Maki, R., Pollock, R.E., Morris, R., Cohen, R., Shankar, A., Blackman, G., et al. (2014). Patient-derived xenografts for individualized care in advanced sarcoma. *Cancer* 120, 2006-2015.
 10. Bello, E., Brich, S., Craparotta, I., Mannarino, L., Ballabio, S., Gatta, R., Marchini, S., Carrassa, L., Matteo, C., Sanfilippo, R., et al. (2019). Establishment and characterisation of a new patient-derived model of myxoid liposarcoma with acquired resistance to trabectedin. *British journal of cancer* 121, 464-473.
 11. Laroche-Clary, A., Chaire, V., Algeo, M.P., Derieppe, M.A., Loarer, F.L., and Italiano, A. (2017). Combined targeting of MDM2 and CDK4 is synergistic in dedifferentiated liposarcomas. *Journal of hematology & oncology* 10, 123.
 12. Bill, K.L., Garnett, J., Meaux, I., Ma, X., Creighton, C.J., Bolshakov, S., Barriere, C., Debussche, L., Lazar, A.J., Prudner, B.C., et al. (2016). SAR405838: A Novel and Potent Inhibitor of the MDM2:p53 Axis for the Treatment of Dedifferentiated Liposarcoma. *Clinical cancer research : an official journal of the American Association for Cancer Research* 22, 1150-1160.
 13. Peng, T., Zhang, P., Liu, J., Nguyen, T., Bolshakov, S., Belousov, R., Young, E.D., Wang, X., Brewer, K., Lopez-Terrada, D.H., et al. (2011). An experimental model for the study of well-differentiated and dedifferentiated liposarcoma; deregulation of targetable tyrosine kinase receptors. *Laboratory investigation; a journal of technical methods and pathology* 91, 392-403.
 14. Qi, Y., Hu, Y., Yang, H., Zhuang, R., Hou, Y., Tong, H., Feng, Y., Huang, Y., Jiang, Q., Ji, Q., et al. (2017). Establishing a patient-derived xenograft model of human myxoid and round-cell liposarcoma. *Oncotarget* 8, 54320-54330.

15. May, C.D., Garnett, J., Ma, X., Landers, S.M., Ingram, D.R., Demicco, E.G., Al Sannaa, G.A., Vu, T., Han, L., Zhang, Y., et al. (2015). AXL is a potential therapeutic target in dedifferentiated and pleomorphic liposarcomas. *BMC cancer* 15, 901.
16. Li, H., Wozniak, A., Sciort, R., Cornillie, J., Wellens, J., Van Looy, T., Vanleeuw, U., Stas, M., Hompes, D., Debiec-Rychter, M., et al. (2014). Pazopanib, a Receptor Tyrosine Kinase Inhibitor, Suppresses Tumor Growth through Angiogenesis in Dedifferentiated Liposarcoma Xenograft Models. *Translational oncology* 7, 665-671.
17. Assi, M., Kenawi, M., Ropars, M., and Rebillard, A. (2017). Interleukin-6, C/EBP-beta and PPAR-gamma expression correlates with intramuscular liposarcoma growth in mice: The impact of voluntary physical activity levels. *Biochemical and biophysical research communications* 490, 1026-1032.
18. Prince, A.C., McGee, A.S., Siegel, H., Rosenthal, E.L., Behnke, N.K., and Warram, J.M. (2018). Evaluation of fluorescence-guided surgery agents in a murine model of soft tissue fibrosarcoma. *Journal of surgical oncology* 117, 1179-1187.
19. Tilkorn, D.J., Al-Benna, S., Hauser, J., Ring, A., Steinstraesser, L., Daigeler, A., Schmitz, I., Steinau, H.U., and Stricker, I. (2012). The Vascularised Groin Chamber: A Novel Model for Growing Primary Human Liposarcoma in Nude Mice. *World journal of oncology* 3, 47-53.
20. Gutierrez, A., Snyder, E.L., Marino-Enriquez, A., Zhang, Y.X., Sioletic, S., Kozakewich, E., Grebliunaite, R., Ou, W.B., Sicinska, E., Raut, C.P., et al. (2011). Aberrant AKT activation drives well-differentiated liposarcoma. *Proceedings of the National Academy of Sciences of the United States of America* 108, 16386-16391.
21. Bi, P., Yue, F., Karki, A., Castro, B., Wirbisky, S.E., Wang, C., Durkes, A., Elzey, B.D., Andrisani, O.M., Bidwell, C.A., et al. (2016). Notch activation drives adipocyte dedifferentiation and tumorigenic transformation in mice. *The Journal of experimental medicine* 213, 2019-2037.
22. Wang, Z., Yang, L., Jiang, Y., Ling, Z.Q., Li, Z., Cheng, Y., Huang, H., Wang, L., Pan, Y., Yan, X., et al. (2011). High fat diet induces formation of spontaneous liposarcoma in mouse adipose tissue with overexpression of interleukin 22. *PloS one* 6, e23737.
23. Fan, Z., Jiang, B., Zhu, Q., Xiang, S., Tu, L., Yang, Y., Zhao, Q., Huang, D., Han, J., Su, G., et al. (2020). Tumor-Specific Endogenous Fe(II)-Activated, MRI-Guided Self-Targeting Gadolinium-Coordinated Theranostic Nanoplateforms for Amplification of ROS and Enhanced Chemodynamic Chemotherapy. *ACS applied materials & interfaces* 12, 14884-14904.
24. Binh, M.B., Sastre-Garau, X., Guillou, L., de Pinieux, G., Terrier, P., Lagace, R., Aurias, A., Hostein, I., and Coindre, J.M. (2005). MDM2 and CDK4 immunostainings are useful adjuncts in diagnosing well-differentiated and dedifferentiated liposarcoma subtypes: a comparative analysis of 559 soft tissue neoplasms with genetic data. *The American journal of surgical pathology* 29, 1340-1347.
25. Chu, W.M. (2013). Tumor necrosis factor. *Cancer letters* 328, 222-225.
26. MacEwan, D.J. (2002). TNF receptor subtype signalling: differences and cellular consequences. *Cellular signalling* 14, 477-492.

27. Oeckinghaus, A., Hayden, M.S., and Ghosh, S. (2011). Crosstalk in NF-kappaB signaling pathways. *Nature immunology* 12, 695-708.
28. Lewis, J.J., Leung, D., Woodruff, J.M., and Brennan, M.F. (1998). Retroperitoneal soft-tissue sarcoma: analysis of 500 patients treated and followed at a single institution. *Annals of surgery* 228, 355-365.
29. Fein, D.A., Corn, B.W., Lanciano, R.M., Herbert, S.H., Hoffman, J.P., and Coia, L.R. (1995). Management of retroperitoneal sarcomas: does dose escalation impact on locoregional control? *International journal of radiation oncology, biology, physics* 31, 129-134.
30. Raut, C.P., and Swallow, C.J. (2010). Are radical compartmental resections for retroperitoneal sarcomas justified? *Annals of surgical oncology* 17, 1481-1484.
31. Fairweather, M., Gonzalez, R.J., Strauss, D., and Raut, C.P. (2018). Current principles of surgery for retroperitoneal sarcomas. *Journal of surgical oncology* 117, 33-41.
32. Tan, M.C., Brennan, M.F., Kuk, D., Agaram, N.P., Antonescu, C.R., Qin, L.X., Moraco, N., Crago, A.M., and Singer, S. (2016). Histology-based Classification Predicts Pattern of Recurrence and Improves Risk Stratification in Primary Retroperitoneal Sarcoma. *Annals of surgery* 263, 593-600.
33. Miao, C., Liu, D., Zhang, F., Wang, Y., Zhang, Y., Yu, J., Zhang, Z., Liu, G., Li, B., Liu, X., et al. (2015). Association of FPGS genetic polymorphisms with primary retroperitoneal liposarcoma. *Scientific reports* 5, 9079.

Figures

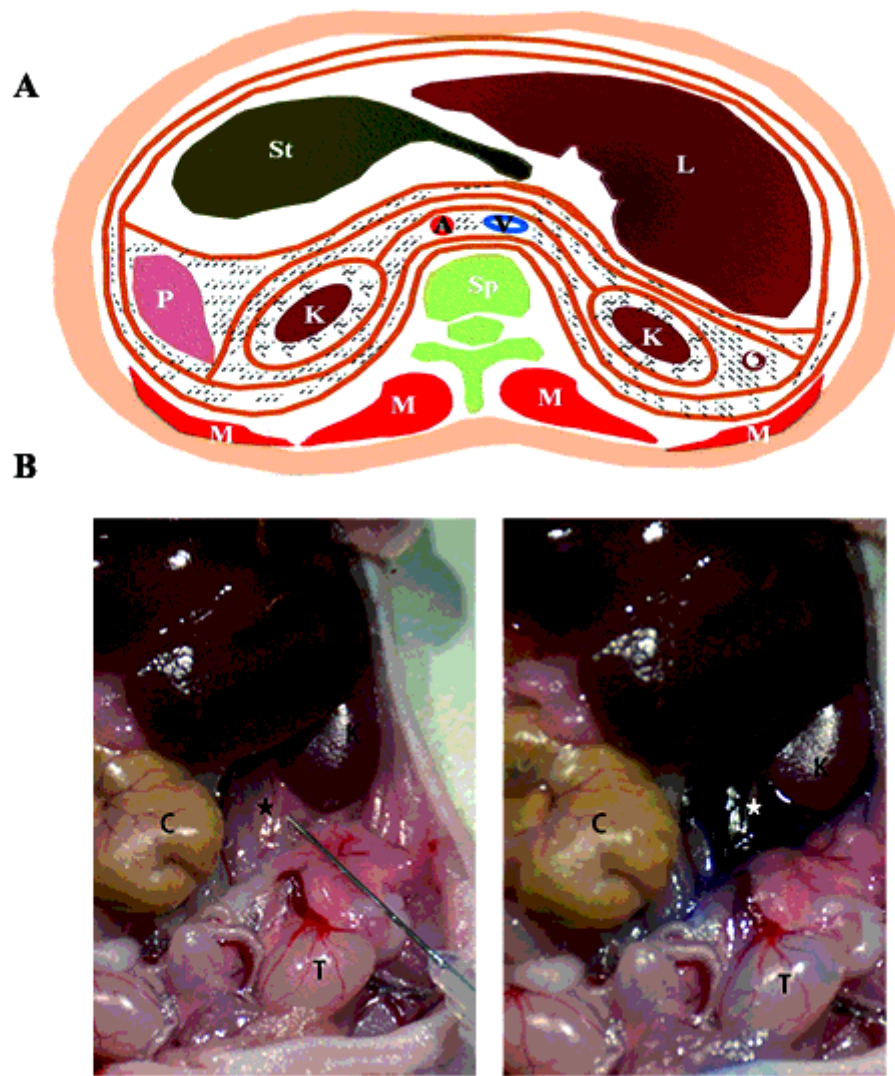


Figure 1

Inoculation of fibrosarcoma HT1080 and liposarcoma SW872 cells into the perirenal space. a: Pattern of retroperitoneal space(L: liver; St: stomach; P: pancreas; K: kidney; Sp: spine; C: colon; M: muscle ; T:testis; spatia retroperitoneaeale; Perirenal space; grafted site); b: Schematic diagram of retroperitoneal sarcoma cell xenografts site . (L: liver; P: pancreas; K: kidney; C: colon; T:testis; grafted site)

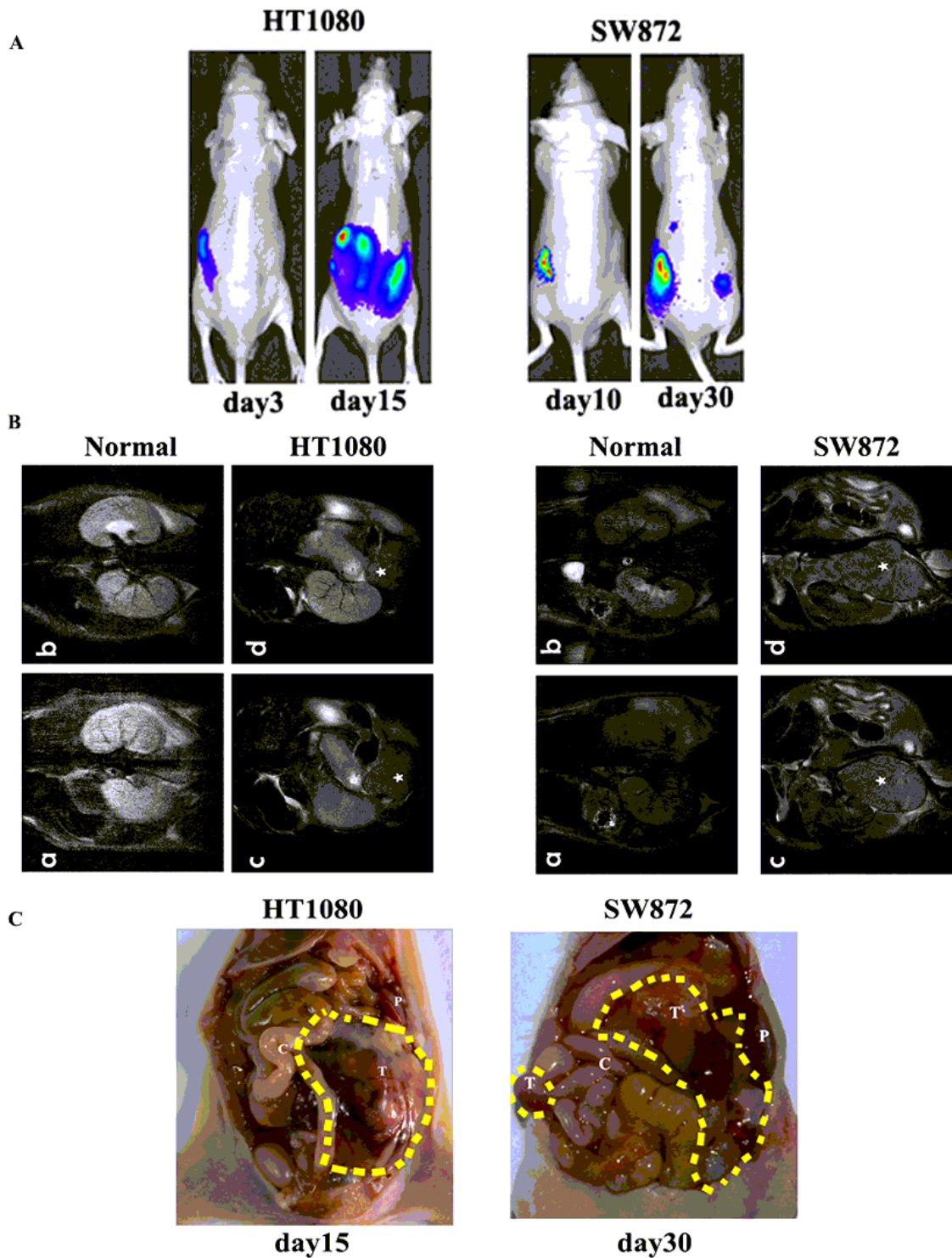


Figure 2

HT1080 and SW872 cells exhibit fast growth and tumorigenesis in the retroperitoneal perirenal space. HT1080 can form a significant solid tumour in the perirenal space within 15 days and SW872 can form a significant solid tumour within 30 days. A: Bioluminescence imaging of HT1080 and SW872 in vivo was carried out; B: In vivo T1-weighted MRI for HT1080 and T2-weighted MRE for SW872 grafted mice, (a,b) control mice; (c,d) tumor-bearing mice; C: Abdominal anatomy of tumor-bearing mice was carried out on

day 15 for HT1080 grafted mice and day 30 for SW872 grafted mice, circle indicate the solid tumor. (P: pancreas; C: Colorectum; T:tumor;K: kidney). For each experiment, a minimum of three mice per group were used, and the results are expressed as average± SD.

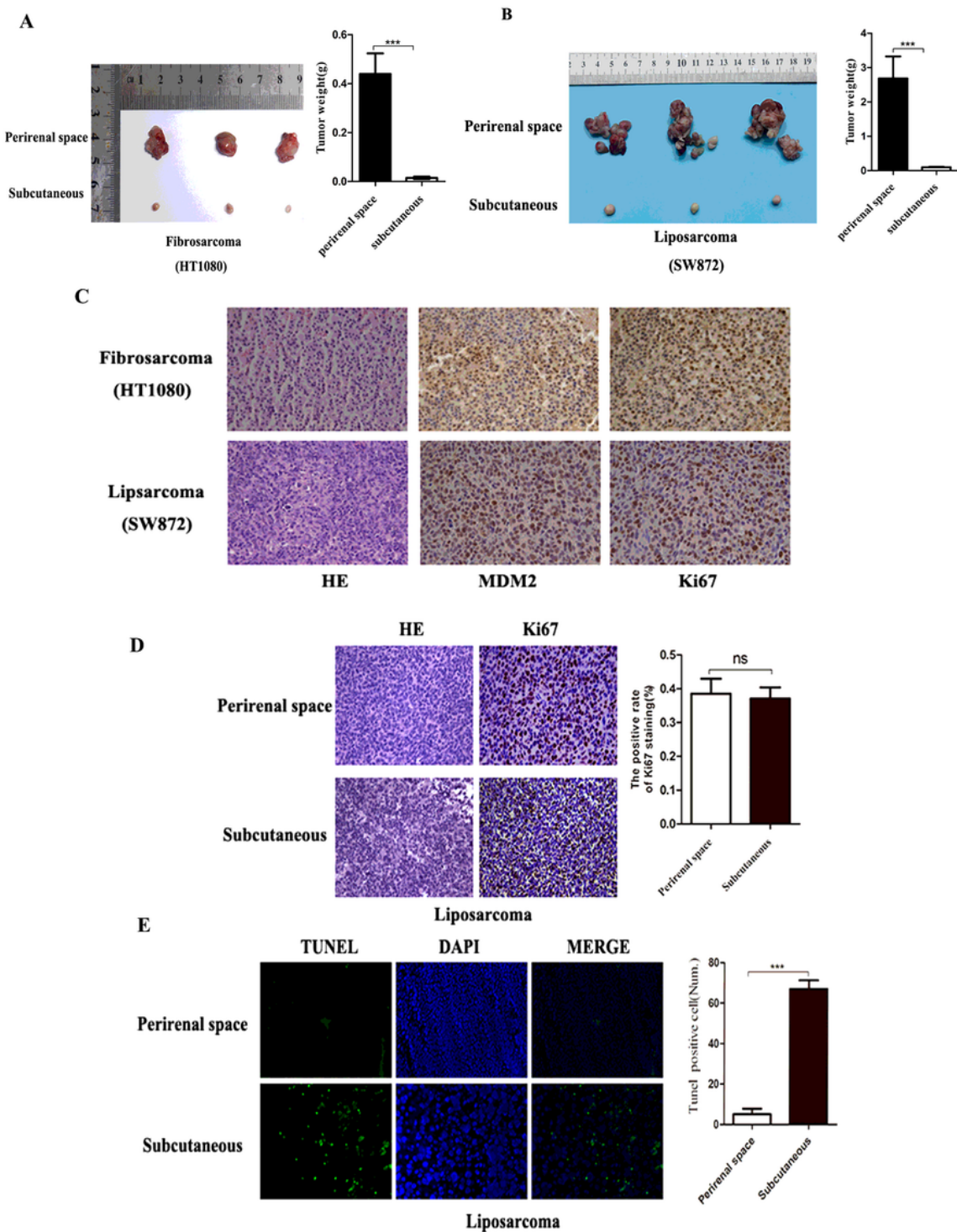


Figure 3

Retroperitoneal sarcoma cells inoculated in the perirenal space have stronger tumorigenic ability than inoculated subcutaneously. A, B:The tumor weight of perirenal space xenograft was significant heavier

than subcutaneous xenograft ($p < 0.001$); C: H&E and IHC staining of implanted human fibrosarcoma cell HT1080 and liposarcoma cell SW872, positive human MDM2 and Ki67 IHC staining was obtained. For each experiment, a minimum of three mice per group were used, and the results are expressed as average \pm SD. D: The positive rate of Ki67 staining in perirenal space xenograft tumor tissue section was no significant difference compared to subcutaneous xenograft tumor. E: Immunofluorescent staining of TUNEL positive cells between perirenal space xenograft and subcutaneous xenograft, The number of TUNEL positive cells in perirenal space xenograft tumor tissue sections was reduced compared with subcutaneous xenograft tumor ($p < 0.001$). For each experiment, a minimum of three mice per group were used, and the results are expressed as average \pm SD. (H&E, x400; MDM2, x400; Ki67, x400)

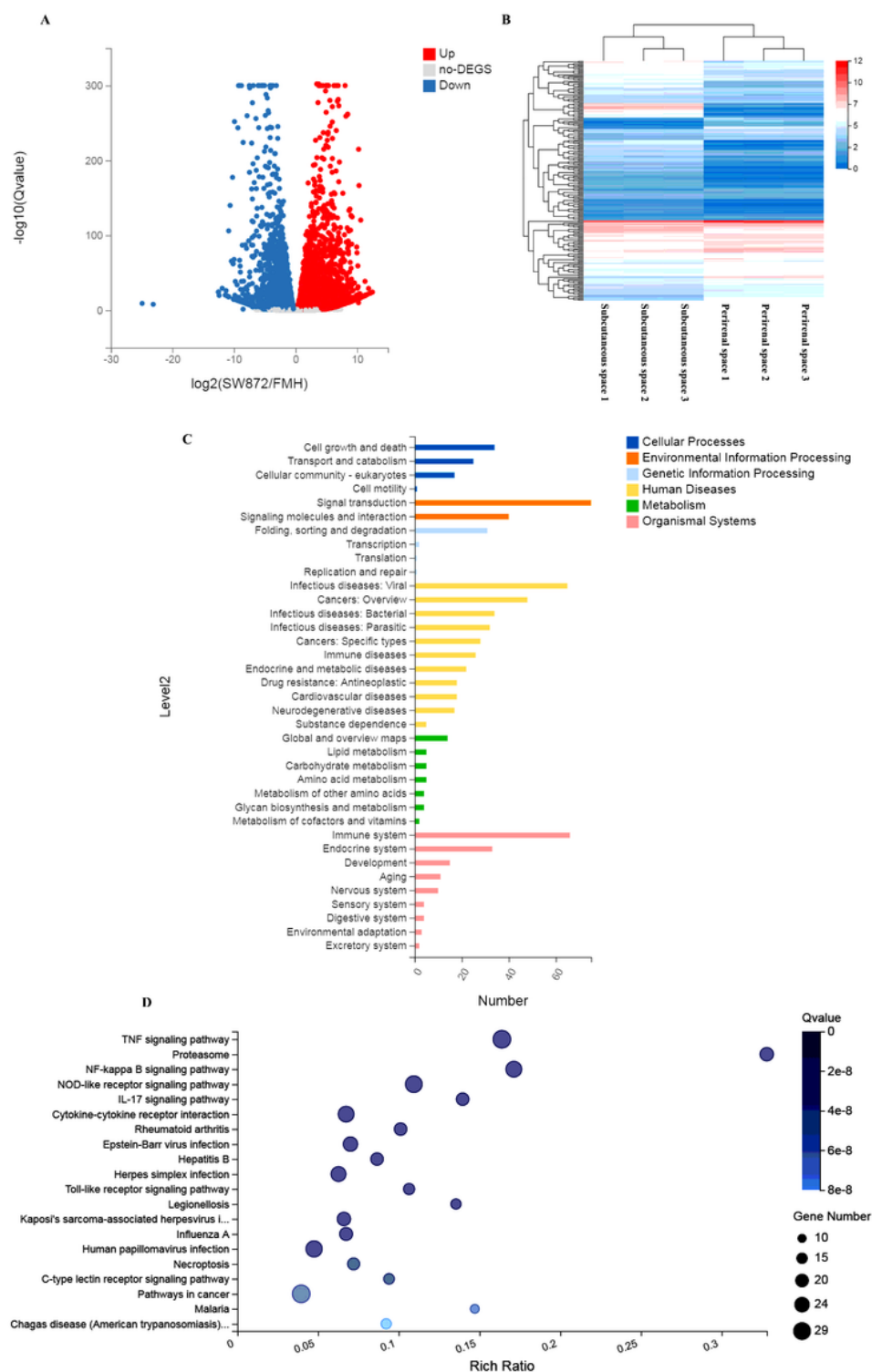


Figure 4

Compare gene expression between perirenal-space-grafted and subcutaneously-grafted tumours A: Volcano plot of DEGs, X axis represent \log_2 transformed fold change, Y axis represents $-\log_{10}$ transformed significance, red points represent up regulated DEG, blue represent down regulated DEG, gray points represent non-DEGs. B: Heat maps showing the frequency of the proteins present in the process of tumorigenesis. C: Pathway functional enrichment of DEGs, X axis represents number of DEGs, Y axis

represents pathway name. D: Enrichment Bubble Diagram of KEGG pathway, X axis represents rich ratio, Y axis represents pathway name, Coloring indicate qvalue (high: blue, low: white), the lower q-value indicate the more significant enriched. Pointsize indicate DEG number (more: big, less: small). For each experiment, a minimum of three mice per group were used, and the results are expressed as average \pm SD.

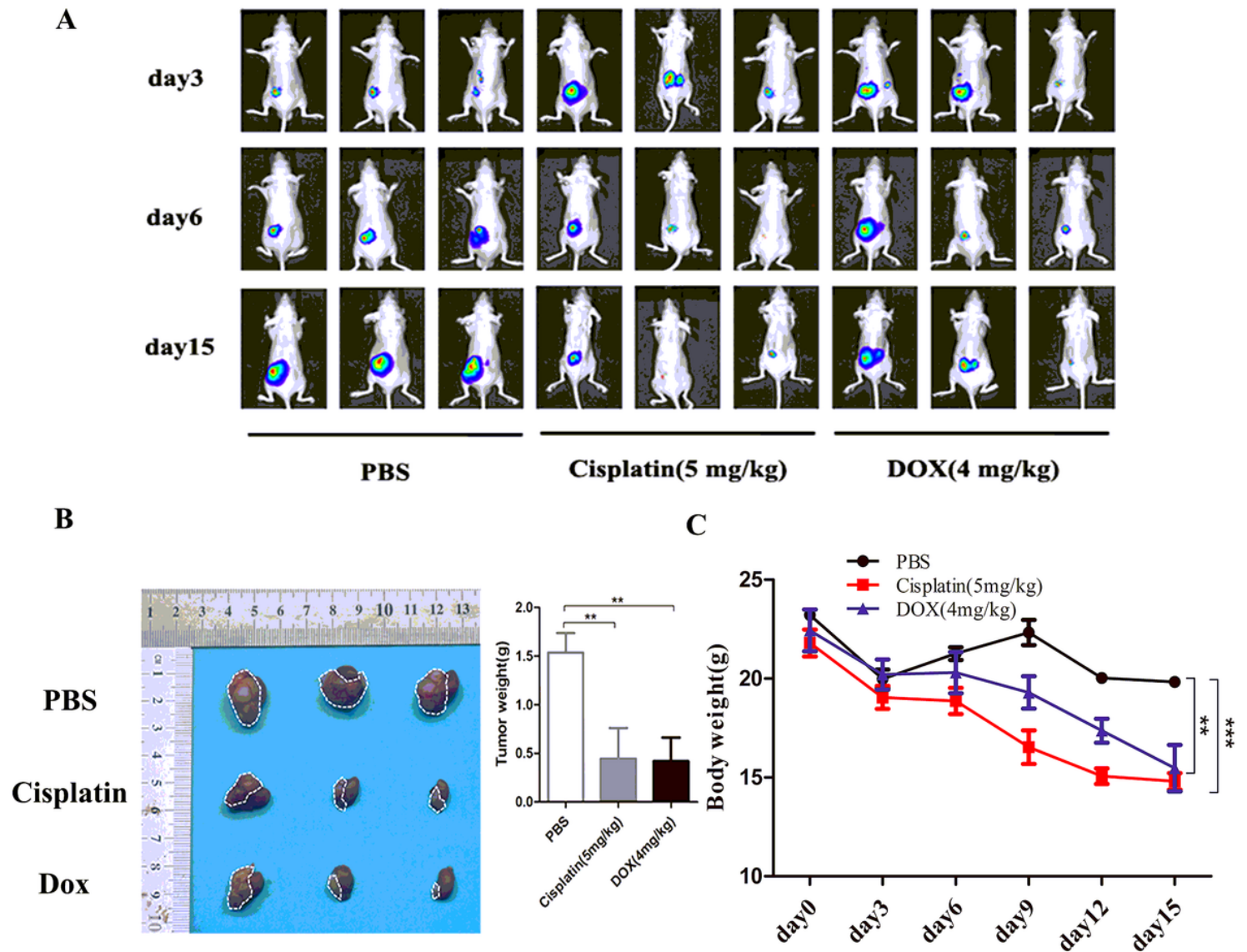


Figure 5

Use perirenal-space-grafted tumorigenesis model to evaluate drug therapies for retroperitoneal sarcoma. A: Bioluminescence signals were collected on the third, the sixth and the fifteenth day after injection. The fluorescence signal of the PBS group increased with time, and higher significantly than cisplatin (5 mg/kg) and DOX (4 mg/kg), B: Nude mice were dissected and solid tumors were weighted. The weight of PBS was significantly higher than that of cisplatin and DOX treated. C: Cisplatin and DOX caused a significant weight loss, of which cisplatin had a greater effect on the weight. For each experiment, a minimum of three mice per group were used, and the results are expressed as average \pm SD.

Supplementary Files

This is a list of supplementary files associated with this preprint. Click to download.

- [Supplementarytable1.xlsx](#)
- [Supplementarytable2.xlsx](#)